Control Engineering Practice 85 (2019) 90–99

Contents lists available at ScienceDirect

Control Engineering Practice

journal homepage: www.elsevier.com/locate/conengprac

Double closed-loop optimal control of greenhouse cultivation

Dan Xu [a,b], Shangfeng Du [c,*], Gerard van Willigenburg [b,*]

[a] Institute of Environment and Sustainable Development in Agriculture, Chinese Academy of Agriculture Sciences, Beijing 100081, PR China
[b] Mathematical and Statistical Methods Group (Biometris), Wageningen University, Droevendaalsesteeg 1, 6708 PB Wageningen, The Netherlands
[c] College of Information and Electrical Engineering, China Agricultural University, Beijing 100083, PR China

ARTICLE INFO

Keywords:
Optimal control
Greenhouse cultivation
Time-scale decomposition
LED lighting
Double closed-loop

ABSTRACT

Two time-scale receding horizon optimal control (TTRHOC) of greenhouse cultivation is investigated. Recent developments enable closure of the outer-loop of this control system because they facilitate on-line recomputation of the optimal control of the slow dynamics on a daily basis. This paper quantifies the benefits obtained from having an outer closed-loop that counteracts errors and changes concerning predictions of crop growth, long-term weather, revenues obtained from selling crops and costs to control greenhouse climate. As a special, important case LED lighting is considered which increases both crop growth and profit. Having an outer closed-loop is especially beneficial in this case.

1. Introduction

Optimal control of greenhouse cultivation has been extensively researched (Gonzalez, Rodriguez, Guzman, & Berenguel, 2014; Seginer, van Straten, & van Beveren, 2017; van Beveren, Bontsema, van Straten, & van Henten, 2015; van Straten, van Willigenburg, van Henten, & van Ooteghem, 2011). Instead of following heuristic set-points, optimal control maximizes profit by exploiting scientific knowledge on greenhouse climate and crops captured in a dynamic greenhouse-crop model. In addition revenues of selling crops and costs associated with greenhouse climate management are considered. Through a two time-scale decomposition (van Henten, 1994; van Henten & Bontsema, 2009), optimal control of greenhouse cultivation is separated into two. One control problem concerns the slow dynamics called "the slow problem" which concerns the control of crop growth during the season. To solve this problem long-term weather predictions are needed. The other control problem is called "the fast problem" and concerns control of the fast dynamics being greenhouse climate. To solve it short-term weather predictions are needed. The separation into two control problems enhances both the accuracy and efficiency of the optimal control computations, thus enabling on-line implementation of a two time-scale receding horizon optimal controller (TTRHOC) (Xu, Du, & van Willigenburg, 2018a,b).

Based on the latest short-term weather predictions and greenhouse climate measurements the TTRHOC repeats optimal control computations concerning the fast greenhouse climate dynamics thus realizing closed-loop control of these in the inner-loop of the TTRHOC. Optimal control of the slow crop dynamics in the outer-loop on the other hand, is usually open-loop. By also repeating optimal control computations of the slow crop dynamics on a daily basis, closed-loop control in the outer-loop of the TTRHOC is realized. Closing both loops of the TTRHOC realizes what will be called a *double closed-loop TTRHOC*. This paper is especially concerned with performance improvements obtained from closing the outer-loop. As shown in this paper, when LED lighting is used in modern greenhouses to promote crop growth (Wang et al., 2017) closing the outer-loop is especially beneficial and important.

The results presented in this paper are entirely based on simulations. Unfortunately, no experimental greenhouse facilities that enable implementation of optimal control were available to the authors of this paper for verification. But all simulations have been selected to closely resemble actual practice or to be conservative.

Long-term predictions of weather, crop growth, revenues obtained from selling crops and costs associated with greenhouse climate management may change significantly during the growing season. By closing the outer-loop, updates and measurements of these are used to counteract associated errors. This is expected to significantly improve performance.

It was recognized by researchers that it is advantageous to repeat optimal control computations concerning the slow dynamics from time to time (van Straten, van Willigenburg, & Tap, 2002). Schmidt et al. (1987) used a simplified discrete-time model of the greenhouse and crop having a time-step of 9 days. As a result they repeated the optimal control computation every 9 days to correct for modelling errors and errors in weather predictions. Effectively these optimal control computations only dealt with a single slow time-scale. Pucheta, Schugurensky, Fullana, Patiño, and Kuchen (2006) used a highly simplified static model for greenhouse climate leaving again just one time-scale concerning control of the slow crop dynamics. They recomputed optimal controls

* Corresponding authors.
E-mail addresses: 13520760485@126.com (S. Du), gerard.vanwilligenburg@wur.nl (L.G. van Willigenburg).

https://doi.org/10.1016/j.conengprac.2019.01.010
Received 16 March 2018; Received in revised form 24 September 2018; Accepted 14 January 2019
Available online xxxx
0967-0661/

using iterative dynamic programming and crop measurements which realize a closed-loop. But they did not compare the performance of an open and closed-loop.

To the best of our knowledge, within the TTRHOC setting, no one ever quantified the benefits brought about by closing the outer-loop i.e. by repeating optimal control computations in the outer-loop on a daily basis using the latest crop measurements and possible changes in weather predictions, crop prices and control costs. The difficulty in solving numerically the optimal control problem of the outer-loop within a TTRHOC setting probably explains this. Recent developments however overcome this difficulty (Xu et al., 2018a,b).

Simulation results of the double closed-loop TTRHOC, presented in this paper, calculate improvements in both profit and crop harvest obtained by closing the outer-loop. Finally the computational effort required by the double closed-loop TTRHOC is investigated to judge the possibility of on-line implementation on a personal computer.

2. Materials and methods

2.1. Greenhouse-crop model

Introduction. Given our aim to simulate and implement a double closed loop TTRHOC on a personal computer, and the fact that even well-established crop models and physical models of the greenhouse lack high accuracy (Ioslovich, Gutman, & Linker, 2009), for both a relatively small white box model is preferred. Such a greenhouse-crop model was presented by van Henten (2003), the crop being lettuce. Because of the increasing need for introducing LED lighting into modern greenhouses (Wang et al., 2017), in this paper the model from van Henten (2003) is extended with LED lighting to also investigate this important case. To facilitate the reading a nomenclature complying with van Henten (2003) describing physical meanings and values of all symbols in this model are presented in Appendix A. The extension of the model is described in the next section while the full model resulting from this is presented in Appendix B.

2.1.1. Modelling of LED lighting

To model LED lighting within the model of van Henten (2003), consider the gross photosynthesis rate $\varphi_{phot,c}$ in this model,

$$\varphi_{phot,c} = \left(1 - e^{-c_{pl,d} X_d}\right) \times \frac{c_{rad,phot} V_{rad} \left(-c_{co2,1} X_T^2 + c_{co2,2} X_T - c_{co2,3}\right)\left(X_c - c_\Gamma\right)}{c_{rad,phot} V_{rad} + \left(-c_{co2,1} X_T^2 + c_{co2,2} X_T - c_{co2,3}\right)\left(X_c - c_\Gamma\right)}. \quad (1)$$

To model the LED lighting the term $c_{rad,phot} V_{rad}$ in Eq. (1) is changed into $c_{rad,phot} V_{rad} + c_{led,phot} U_l$, with $c_{led,phot}$ being LED light use efficiency and control input U_l being electric power generating LED light. According to van Henten (1994), $c_{rad,phot}$ is given by,

$$c_{rad,phot} = \varepsilon c_{par} c_{rad,rf}. \quad (2)$$

In Eq. (2), $\varepsilon = 17\ 10^{-9}$ kg J^{-1} is light use efficiency, $c_{par} = 0.5$ is the ratio of photosynthetically active radiation to total solar radiation, $c_{rad,rf} = 0.42$ is the solar radiation transmission coefficient of the roof. Similarly,

$$c_{led,phot} = \varepsilon c_{par} \eta_{led}. \quad (3)$$

In Eq. (3) η_{led} represents efficiency of energy transfer from electricity to LED light. Combining results from Heuvelink and Challa (1989), who consider HPS lighting, and Singh, Basu, Meinhardt-Wollweber, and Roth (2015) who compare this with LED lighting, that is 4 times as efficient and used in this paper, $\eta_{led} = 0.736$ is obtained. Accordingly $c_{led,phot} = 6.256\ 10^{-9}$ kg J^{-1}. Assuming installation of one LED light (400 W) per m^2 greenhouse $0 \le U_l \le 400$ W m^{-2}. The extended full model is presented in Appendix B.

Table 1
Bounds on greenhouse state variables.

State variable	X_c (kg m^{-3})	X_T (°C)	R_{Xh} (kg m^{-3})
Upper bound	2.75 10^{-3}	40.0	0.9
Lower bound	0	6.5	0

Table 2
Bounds on control inputs.

Control input	U_c (kg m^{-2} s^{-1})	U_q (W m^{-2})	U_v (m s^{-1})	U_l (W m^{-2})
Upper bound	1.2 10^{-6}	150	7.5 10^{-3}	400
Lower bound	0	0	0	0

2.2. Control objective and control problem constraints

The economic performance measure is selected to be profit, which is maximized by the optimal control. The specification of profit P is taken from van Henten (2003) and extended with costs associated with LED lighting and mechanical ventilation,

$$P = c_{pri,1} + c_{pri,2} X_d\left(t_f\right) - \int_{t_0}^{t_f} \left(c_{CO_2} U_c(t) + c_q U_q(t) + c_v U_v(t) + c_{el} U_l(t)\right) dt. \quad (4)$$

Running costs of mechanical ventilation by a ventilation fan are represented by $c_v U_v(t)$ and of LED lighting by $c_{el} U_l(t)$ in Eq. (4). Parameter value $c_v = 2.226\ 10^{-6}$ \$ m^{-3} is based on the ratio of cost associated with mechanical ventilation and CO_2 supply as specified by Ioslovich (2009). Parameter value $c_{el} = 2.5\ 10^{-8}$ Hfl J^{-1} is found from Heuvelink and Challa (1989). Considering the old Dutch currency Hfl has disappeared, an exchange rate of 0.53 from Hfl to American dollar \$ applies to determine the current economic value. Therefore $c_{el} = 1.325\ 10^{-8}$ \$ J^{-1}.

The greenhouse-crop model does not describe the effect of extreme climate conditions on crop growth and crop diseases. Its range is limited to climate conditions that are considered acceptable for ordinary crop growth. Therefore climate state variables are upper and lower bounded. These bounds reflect what are considered acceptable growth conditions. They are recorded in Table 1, where R_{Xh} is relative humidity. In addition there are bounds on all control inputs, determined by the control equipment. These are recorded in Table 2.

2.3. Two time-scale receding horizon optimal control system

2.3.1. Overview and block diagram

Time-scale decomposition within optimal control of greenhouse cultivation was introduced by van Henten (1994), see also van Henten and Bontsema (2009), van Straten et al. (2011) and Xu et al. (2018a,b). A block diagram of the two time-scale receding horizon optimal control system is shown in Fig. 1. In Fig. 1 x_s in the outer-loop represents the "slow states", i.e. the state vector containing all states of the slow problem, which in our case is just X_d. Furthermore λ_s is the corresponding "slow co-state". Similarly $\boldsymbol{x_f}$ in the inner-loop represents the "fast states", i.e. the state vector containing all fast states representing the greenhouse climate. For further details refer to Appendix B. From Fig. 1 observe that the main extension of the original scheme of van Henten (1994) is the introduction of control input U_l.

The receding horizon optimal controller (RHOC) in the inner-loop controls the fast states $\boldsymbol{x_f}$ representing the greenhouse climate. In addition it requires the state x_s and co-state λ_s obtained from the slow problem, i.e. the optimal control computation in the outer-loop. The co-state λ_s equals the marginal value of crop dry weight that determines partly the cost function used by the RHOC in the inner-loop.

The outer-loop uses the crop state and a long-term weather prediction to compute the optimal control that maximizes profit as represented by Eq. (4). This optimal control computation is performed at least once,

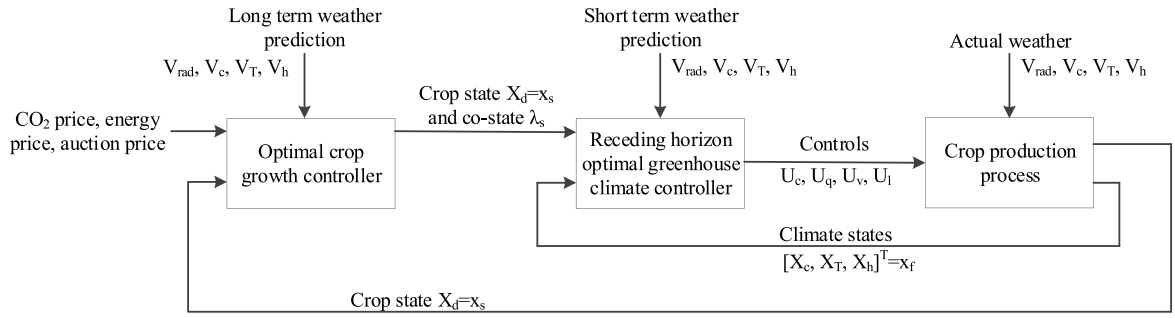

Fig. 1. Two time-scale receding horizon optimal control system.

at the start of the season, for the entire growing season. But it may be repeated several times during the growing season to enhance accuracy (van Henten, 1994; van Straten et al., 2002). This enables the use of *measurements* of crop dry weight, as well as *updates* of long-term weather predictions and prices involved in the outer-loop. Doing so realizes the double closed-loop TTRHOC that is implemented and simulated in this paper to investigate and quantify possible improvements obtained from closing the outer-loop. In addition the possibility of real-time implementation of the double closed-loop TTRHOC on a personal computer is investigated.

2.3.2. Optimal control of crop growth in the outer-loop

The optimal control computation in the outer-loop of Fig. 1 requires a long-term slowly varying weather prediction for the entire growing period as well as prices for heating energy, CO_2 supply, ventilation, in some cases LED lighting, and selling harvested crops as described in Section 2.2. The long-term weather prediction is a smoothed version of hourly recorded weather data from 1989, which is the reference year for Dutch (49–53 °N, 3–7 °E) greenhouses (Breuer & van de Braak, 1989). V_T, V_h, and V_{rad} are taken from the first 50 days (January and part of February) of 1989. For V_c a fixed value is assumed because it varies little during the day. These data are depicted in Fig. 2.

Some expected trends are clearly seen from these data. The solar radiation usually reaches its maximum at midday. Humidity and temperature trends are clearly related, because water vapour saturation pressure is closely related to temperature.

Taking the long-term weather prediction to be just data taken from an earlier, similar period, may seem not to be the best choice. But alternatives, especially on a term of months, are not easily obtained. Still current commercial weather predictions over one or two weeks appear to be better than the data from an earlier, similar period. So improving long-term weather predictions is certainly worth further investigation.

The optimal control computations are performed using Matlab optimal control software called PROPT (Ross & Fahroo, 2004; Rutquist & Edvall, 2010) that is very efficient. Applying the two time-scale decomposition, the optimal control computation in the outer-loop considers the greenhouse dynamics to be static. Details of this are found in Appendix C and in Xu et al. (2018a) in which similar TTRHOC computations are described and performed.

Recomputation of the seasonal optimal control in the outer-loop is performed at the start of each day taking the optimal control from the previous computation as the initial guess. The horizon of the seasonal optimal control runs from the current day until the last day of the growing season after which the lettuce crop is harvested and sold.

2.3.3. Receding horizon optimal control of greenhouse climate in the inner-loop

The RHOC in the inner-loop is an on-line digital optimal controller with a sampling period of 2 min and a control horizon of 1 h. Since solar radiation may change within minutes and significantly influences control, while inner-loop optimal control computations always finish within 2 min, 2 min was selected as the sampling period. The control horizon of 1 h relates to a study of the very simple lazy man weather prediction, that simply uses the latest measurements as the weather prediction. This study (Tap, Van Willigenburg, & Van Straten, 1996) shows that the lazy man weather prediction is still hard to beat within a time-span of 1 h. In recomputing digital optimal controls over the control horizon of 1 h a sampling period of 20 min was used. As compared to the real sampling period of 2 min, this increases the sensitivity of the performance to the first control input, which is the only one applied by the RHOC. Further details concerning these choices can be found in van Willigenburg, van Henten, and van Meurs (2000). The cost function J_{RHOC}, to be minimized by the RHOC, is given by,

$$J_{RHOC} = \int_{t_0}^{t_f} \left(c_q U_q(t) + c_{CO_2} U_c(t) + c_v U_v(t) + c_{el} U_l(t) \right) - \lambda_s^T f_s\left(x_s, \boldsymbol{x_f}, \boldsymbol{u}\right) dt. \quad (5)$$

The cost function in Eq. (5) contains the slow crop state $x_s = X_d$ as well as the "slow" co-state λ_s as represented by Fig. 1. Both are obtained from the optimal control computation in the outer-loop. Both x_s and λ_s must be stored in the RHOC controller memory. Further details concerning the optimal control computation in the inner-loop that uses a so called 'lazy man' weather prediction can be found in Xu et al. (2018b).

3. Results and discussion

3.1. Introduction

During a growing season, long-term predictions of weather, crop growth and crop selling price and costs of control, generally change. To better handle these changes the benefits of re-computing optimal controls in the outer-loop, based on the latest information and measurements, is investigated. Two different cases will be considered. One with, and one without LED lighting. Finally feasibility of on-line implementing the proposed double closed-loop TTRHOC on a personal computer is investigated.

3.2. Closing the outer-loop with a static inner-loop

To get a first impression of possible benefits obtained from closing the outer-loop, Table 3 presents profit and crop dry weight computed using perfect and erroneous predictions of solar radiation, price of the crop and costs associated with control, as indicated by the first column in Table 3. For example, the second line in Table 3 assumes perfect long-term predictions except for the solar radiation which is predicted to be only 50% of the true value. The optimal control computed from these predictions is applied to the greenhouse (model) subjected to solar radiation having its true value (which is 50% higher than the predicted one). The profit and crop harvest obtained in this manner are recorded in column 2 and 3 of Table 3. The percentages recorded in between brackets indicate the difference with the perfect value on top of columns 2 and 3, obtained when predictions are all perfect.

Since profit is maximized, compared to the case of perfect predictions on top of columns 2 and 3, one might always expect a decrease of

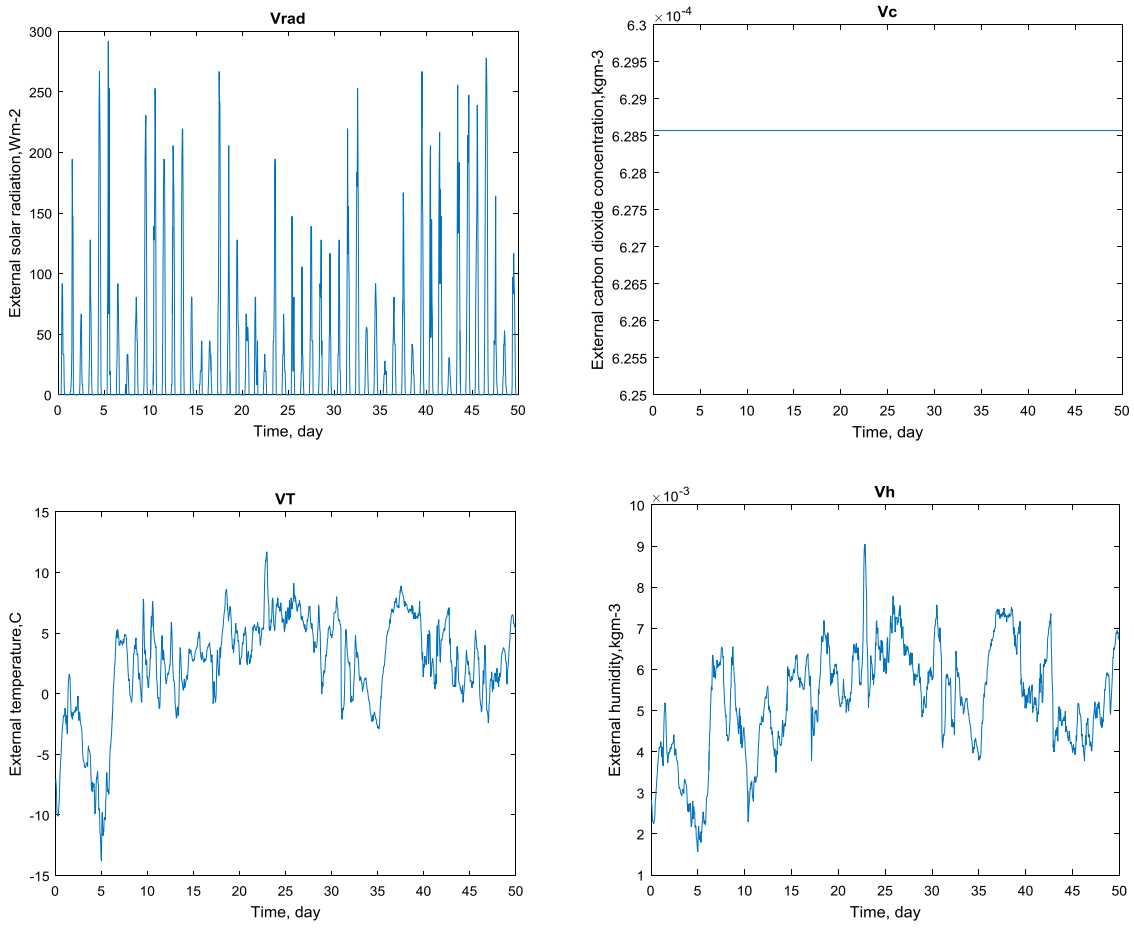

Fig. 2. External weather data over the entire growing season of 50 days.

Table 3
Effect of long-term prediction errors.

Long-term prediction	Profit ($ m^{-2})	Crop (kg m^{-2})
Perfect	1.6637	0.1352
50% solar radiation	1.4364 (−13.66%)	0.1031 (−23.74%)
150% solar radiation	1.6823 (+1.12%)	0.1409 (+4.22%)
50% crop price	1.6141 (−2.98%)	0.1255 (−7.17%)
150% crop price	1.6606 (−0.19%)	0.1366 (+1.04%)
50% control costs	1.6483 (−0.93%)	0.1369 (+1.26%)
150% control costs	1.6429 (−1.25%)	0.1307 (−3.33%)

profit. But this is not so on the third line of Table 3 because of state constraints taking preference over maximizing profit. In the case of over-estimated solar radiation (150%) in Table 3 the computed optimal control, when applied to the real system, improves profit by 1.12% but at the expense of violating state constraints. In the case of under-estimated solar radiation (50%) state constraint violation also occurs. The latter indicates the importance of accurate weather predictions in satisfying state constraints. Also it shows that the results in Table 3 must be interpreted with care. We finally remark that all optimal control computations and simulations resulting in Table 3 considered the fast greenhouse dynamics to be static, as described in Appendix C.

As crop prices and control costs do not directly influence the violation of state constraints, erroneous predictions of them will never lead to state constraint violations as long as the weather predictions and crop dry weight are perfectly predicted, as in the last four rows of Table 3. When the crop selling price is underestimated (50% crop price), as expected, savings on control costs and less harvested crop dry weight (−7.17%) are obtained and vice versa. When the control costs are underestimated (50% control costs), as expected, additional control costs and harvested crop dry weight (+1.26%) are obtained and vice versa.

Taking the above results and arguments into consideration, as to maximizing profit, Table 3 still provides a first indication of what may be gained and lost by closing the second loop. Solar radiation appears to be dominant (−13.66% at most) which complies with van Henten (2003). The effect of changes in crop price and control costs is significantly less (no more than 2.98% in the last 4 rows).

3.3. Outer open-loop and inner closed-loop TTRHOC

Assuming a static inner-loop, as in the previous section, is an *approximation* and excludes the feedback of measured climate variables occurring in the inner-loop of Fig. 1. This feedback may significantly compensate for errors in long-term weather predictions used in the outer-loop. The dynamics of the inner-loop imply that state constraints have to be satisfied on the corresponding fast time-scale, whereas in the outer-loop they only have to be satisfied on the corresponding slow time-scale. As a result the inner-loop realizes values of crop dry weight $x_s = X_d$ that differ from those computed off-line at the start of the season in the outer-loop. Closing the outer-loop by feeding back daily these computed values of crop dry weight in the inner-loop, is thus expected to also improve performance in actual practice. The inner-loop uses a short-term weather prediction. Motivated by Tap (2000) the 'lazy man' weather prediction is used in the inner-loop. This prediction simply assumes the short-term weather to be equal to the latest local weather measurements. It realizes feedback of local weather measurements to counteract errors in long-term weather predictions.

From the previous section prediction errors of solar radiation in the outer-loop turned out dominant for performance degradation. Therefore

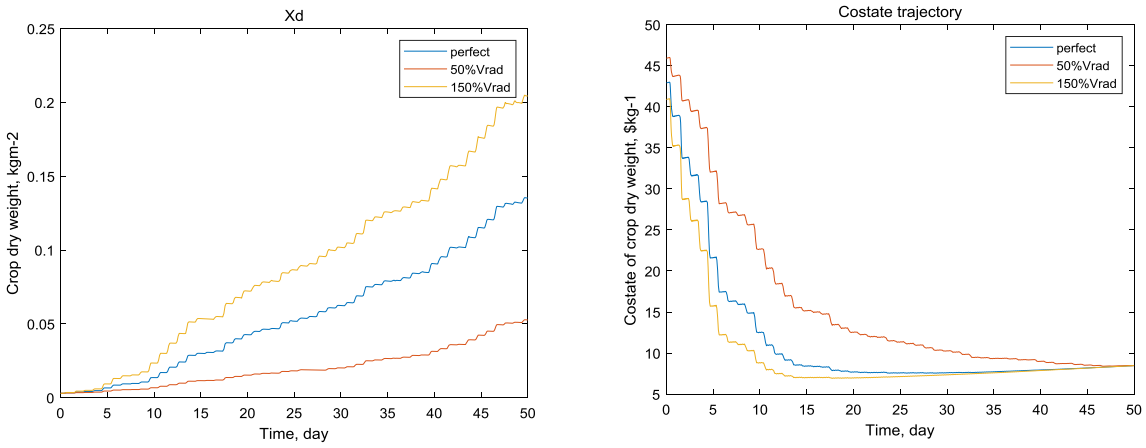

Fig. 3. Optimal state and co-state trajectories of the slow problem.

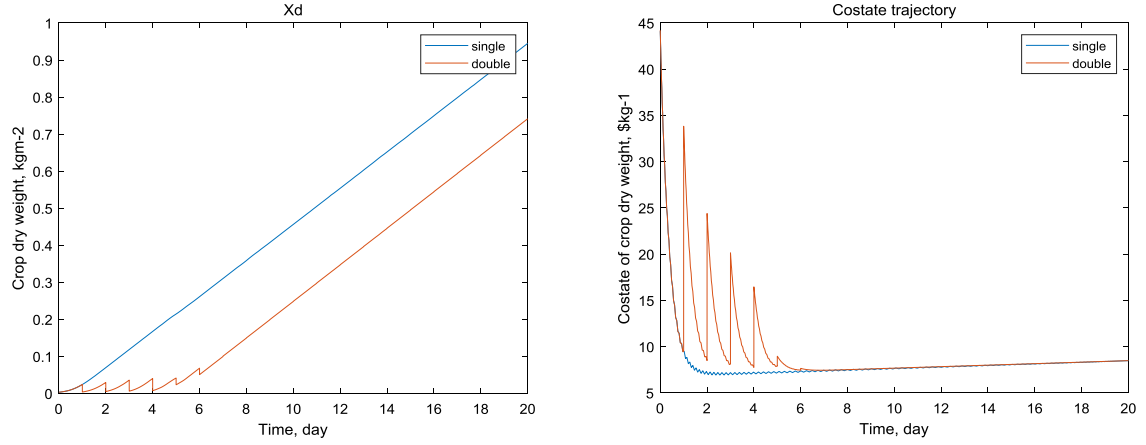

Fig. 4. Optimal state and co-state trajectories of the slow problem with LED lighting. (For interpretation of the references to colour in this figure legend, the reader is referred to the web version of this article.)

Table 4
Counteracting long-term errors in single closed-loop TTRHOC.

Long-term prediction	Profit ($ m^{-2})	Crop (kg m^{-2})
Perfect	1.5619	0.1200
50% solar radiation	1.5307 (−1.99%)	0.1154 (−3.83%)
150% solar radiation	1.5604 (−0.096%)	0.1196 (−0.33%)

in this section only cases of erroneous predictions of long-term solar radiation will be considered. Table 4 records profit and crop dry weight when the inner-loop is closed while the single computation in the outer-loop (open outer-loop) uses perfect and erroneous predictions of solar radiation as mentioned in the first column.

Table 4 considers the dynamics of the inner-loop whereas Table 3 uses a static approximation of the inner-loop. Comparing the first rows of Tables 3 and 4, profit decreases with 6.12% and crop dry weight with 11.24%. Not considering fast dynamics explicitly, as well as the associated state constraints satisfaction, results in too optimistic values of profit and crop dry weight in Table 3.

Optimal state and co-state trajectories of the slow problem, computed under perfect and erroneous predictions of solar radiation in the outer-loop, are shown in Fig. 3. Their relative differences are significant. But when transferred into the inner-loop in Fig. 1, through the cost function in Eq. (5), the relative differences of profit in Table 4 are very much smaller. This is explained by the feedback of measurements of greenhouse climate as well as weather conditions that make up the 'lazy man' weather prediction in the inner-loop. Given the relatively small differences in Table 4, closing the outer-loop does not lead to significant improvement of profit. When LED lighting is realized in the greenhouse, closing the outer-loop is much more beneficial, as demonstrated in the next section.

3.4. Double closed-loop TTRHOC with LED lighting

Lettuce crops can grow properly under continuous light (Dorais & Gosselin, 2000; Velez-Ramirez, van Ieperen, Vreugdenhil, & Millenaar, 2011) so LED lighting can significantly enhance lettuce crop growth. By applying it Lin et al. (2013) showed that lettuce can be harvested after 20 instead of 50 days. To incorporate LED lighting the model of van Henten (2003) was modified as described in Section 2.1.1, as well as the associated control objective as described in Section 2.2. Fig. 4 shows optimal state and co-state trajectories of the slow problem for two different cases namely single and double closed-loop TTRHOC. In both cases all predictions in the outer-loop are assumed to be perfect. The blue lines indicate the single closed-loop case where the inner-loop is closed while the outer-loop is open. The blue lines thus represent the result of a single slow problem computed at the start of the growing season of 20 days. The red lines represent the double closed-loop case in which both the inner and outer-loop in Fig. 1 are closed. The outer-loop is recomputed each single day and the red lines only show the result for the next day which is the only part applied to the real system. This explains the jumps that occur, especially at the start of the season during the first 6 days.

Thus, despite the fact that perfect predictions are assumed in the outer-loop, recomputation of the outer-loop after each single day shows significant changes, especially during the first 6 days of the growing

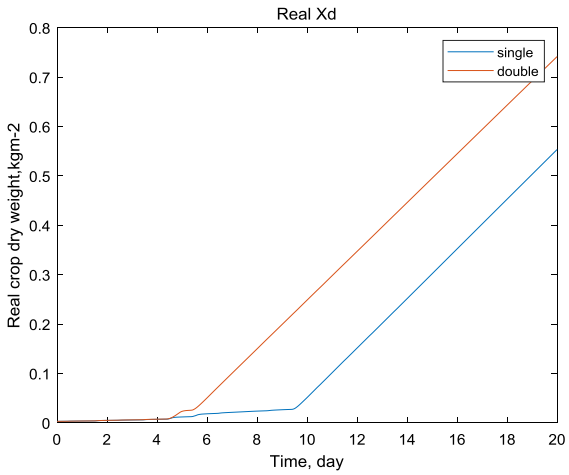

Fig. 5. Crop growth as obtained from single and double closed loop TTRHOC with LED lighting.

Table 5
Profit and crop harvest of single and double closed-loop TTRHOC.

RHOC	Profit ($ m^{-2})	Crop (kg m^{-2})
Single closed-loop TTRHOC	1.9475	0.5534
Double closed-loop TTRHOC	2.4247 (24.50%)	0.7416 (34.01%)

season. This is explained by the phenomena described at the start of Section 3.3. The main phenomenon being satisfaction of state constraints at the small time-scale that is not incorporated in the slow problem of the outer loop. State constraints at the small time-scale are mostly realized by the inner-loop at the expense of profit and crop growth as *calculated* in the outer-loop. Therefore the *real* crop weight depicted in Fig. 5, obtained from the inner-loop computation that takes into account the fast dynamics and constraint violations, is significantly less, especially during the first 6 days. By closing the outer-loop the crop dry weight $x_s = X_d$, which is computed through the crop growth model, measurement data of greenhouse climate and external weather collected during RHOC and possibly measurements of crop dry weight, is fed back thus correcting significantly the state and co-state trajectory of the slow problem in the outer-loop, especially during the first 6 days. As to the magnitude of these corrections, note that the co-state λ_s of the slow problem is precisely the sensitivity of the optimal performance to increments in $x_s = X_d$. So the corrections are roughly proportional to λ_s as can be seen from Fig. 4. Profit and harvested crop dry weight are recorded in Table 5 for both single and double closed-loop TTRHOC showing the significant improvement of closing the outer- loop in Fig. 1.

Comparing the last row of Table 5 with the first row in Table 4, one can see a 55.24% increase in profit, as well as a 518% increase in crop harvest obtained from adding LED lighting and closing the outer-loop in Fig. 1, while reducing the growing season from 50 to 20 days. One should note that the drastic increase in crop harvest is mainly caused by LED lighting, which keeps the crop growing at a high rate during day and night. Comparing our results with Engindeniz and Tuzel (2006), who reported 0.55–0.63 kg m^{-2} crop dry weight harvest (11.56–12.30 kg m^{-2} crop fresh weight), even without LED lighting, the calculated crop harvest is a reasonable amount. Note that the increase in profit is not proportional to that in crop harvest because running costs as given in Eq. (4) also increase, especially those related to LED lighting. Compared with Fig. 3, the optimal state and co-state trajectory of the slow problem in Fig. 4, apart from discontinuities due to daily feedback in the outer-loop, are much more smooth. This is because, as opposed to Fig. 3, in Fig. 4 optimal control includes LED lighting that also realizes crop growth during night time, as shown by Fig. 6.

As shown in an experiment by Martineau, Lefsrud, Naznin, and Kopsell (2012), lettuce cultivation for 28 days with LED lighting (81.8

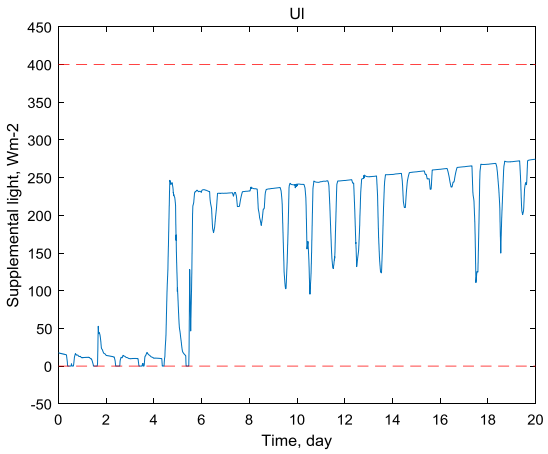

Fig. 6. LED lighting.

Table 6
Computation time on a PC.

RHOC	Outer-loop	Inner-loop
50 days without LED	30 min	10 s
20 days with LED	5 min	40 s

W m^{-2}) for 10.5 h each day consumed 0.866 10^8 J m^{-2} electricity and produced 0.142 kg m^{-2} crop dry weight. A profit of 1.147 $ m^{-2} can be calculated with the price $c_{pri,1}$, $c_{pri,2}$, and c_{el} given in (4). This number compares with those of profit shown in Table 5, and provides the further improvement brought about by adding optimal control to LED lighting.

Finally, to see the strict state constraint satisfactions realized by the inner-loop, Fig. 7 shows the greenhouse climate states representing the fast time-scale. From Fig. 7 one can also see the increase in both CO_2 concentration and temperature to promote photosynthesis rate since day 6. The latter matches the conclusion of Ioslovich (2009) stating it is not advisable to apply supplemental lighting at an early stage of crop growth.

3.5. Computation time

To investigate the possibility of implementing the proposed double closed-loop TTRHOC, average computation times obtained on a commercial PC (CPU: i7-6700HQ @2.6 GHz, RAM: 8GB) are shown in Table 6. Given the 1-day update rate of the outer-loop and the 2-minute update rate of the inner-loop, on-line implementation on a personal computer is feasible in all cases. Given the benefits brought about by LED lighting, as computed in Section 3.4, as well as the ability to implement the associated double closed-loop TTRHOC, as confirmed by Table 6, the use of both is highly recommended. One should note that the improvement of PC computing power and development of efficient optimal control software together facilitates the possibility of on-line implementation.

4. Conclusions

Profit as obtained from lettuce cultivation in greenhouses may largely benefit from LED lighting combined with a double closed-loop, two time-scale, receding horizon optimal control system (double closed-loop TTRHOC). Optimal control computations and simulations of this combination, presented in this paper, have demonstrated this. They show a 55% increase in profit and a 518% increase in crop harvest, while reducing the cultivation period to 20 days.

The initial objective of this research was actually to investigate benefits of closing the outer-loop of a two time-scale receding horizon optimal control system (TTRHOC) for lettuce cultivation in greenhouses. Closing the outer-loop comes down to a daily recomputation of the slow

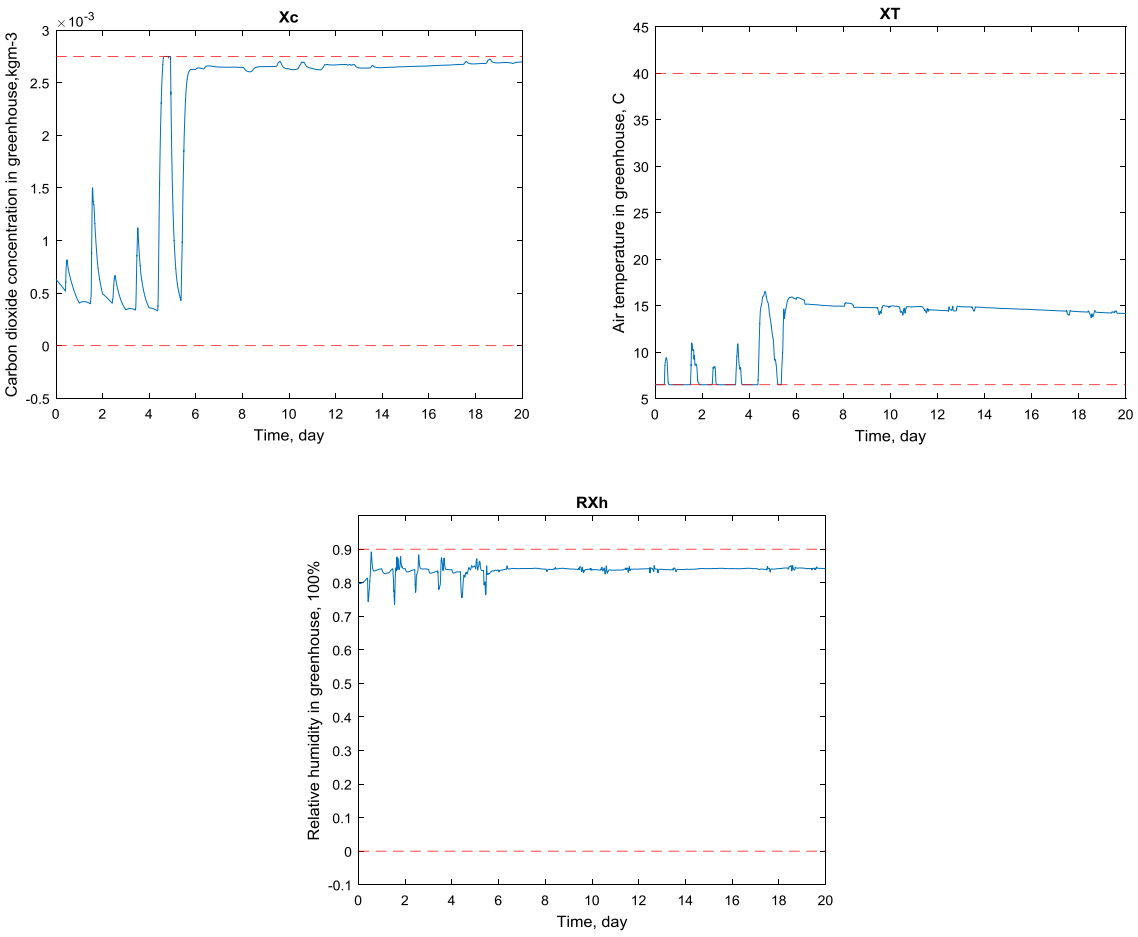

Fig. 7. Fast states.

problem, which in a conventional TTRHOC, is solved only once at the start of the growing season. Closing the outer-loop realizes feedback of computations or estimates of crop dry weight in the inner-loop. The computation of crop dry weight in the inner-loop differs significantly from the long-term computation at the start of the season. Apart from erroneous long-term estimates of weather and prices of controls and lettuce crop, used by the outer-loop, this occurs because of the fast dynamics and state constraint satisfaction in the inner-loop. The latter are approximated, and therefore partly violated, in the outer-loop. Especially in the case of LED lighting and especially at the start of the growing season, closing the outer-loop by feeding back crop dry weight from the inner-loop, leads to significant improvement of economic performance and crop harvest. Without LED lighting, by closing the outer-loop, profit is increased by no more than 2.98% (Table 3) in our computations. With LED lighting an increase of 24.5% (Table 5) in profit was computed.

The possible real-time implementation on a personal computer of the double closed-loop TTRHOC was also investigated. By exploiting advanced optimal control software, real-time implementation of optimal control computations in both the inner and outer-loop of the TTRHOC turns out feasible when the update rates of these loops are 2 min and 1 day respectively.

Conflict of interest

None declared.

Acknowledgements

The discussions with Eldert van Henten, Bert van Ooster and Rachel van Ooteghem have largely contributed to the ripening of ideas in this paper. This work was financially supported by the China Scholarship Council - China (201506350209).

Appendix A. Nomenclature (complies with van Henten, 2003)

Symbol	Physical meaning	Value	Unit
$c_{ai,ou}$	heat transmission coefficient through the greenhouse cover	6.1	W m^{-2} °C^{-1}
$c_{rad,phot}$	solar light use efficiency	3.55 10^{-9}	kg J^{-1}
$\varphi_{phot,c}$	gross canopy photosynthesis rate		kg m^{-2} s^{-1}
$c_{pl,d}$	effective canopy surface	53	m^2 kg^{-1}
X_d	crop dry weight		kg m^{-2}
V_{rad}	solar radiation outside the greenhouse		W m^{-2}
X_T	air temperature in the greenhouse		°C
X_c	carbon dioxide concentration in greenhouse		kg m^{-3}
c_Γ	carbon dioxide compensation point	5.2 10^{-5}	kg m^{-3}

Symbol	Physical meaning	Value	Unit
$c_{co2,1}$	temperature effect on CO_2 diffusion in leaves	5.11 10^{-6}	m s^{-1} °C^{-2}
$c_{co2,2}$	temperature effect on CO_2 diffusion in leaves	2.30 10^{-4}	m s^{-1} °C^{-1}
$c_{co2,3}$	temperature effect on CO_2 diffusion in leaves	6.29 10^{-4}	m s^{-1}
U_l	electric power for generating LED light		W m^{-2}
$c_{led,phot}$	supplemental artificial light use efficiency	6.256 10^{-9}	kg J^{-1}
ϵ	light use efficiency	17 10^{-9}	kg J^{-1}
c_{par}	ratio of photosynthetically active radiation to total solar radiation	0.5	
$c_{rad,rf}$	transmission coefficient of the roof for solar radiation	0.42	
η_{led}	transfer efficiency of electricity to LED light	0.736	
t	time		S
X_h	humidity concentration in greenhouse		kg m^{-3}
$c_{\alpha\beta}$	yield factor	0.544	
$c_{resp,d}$	respiration rate in terms of respired dry matter	2.65 10^{-7}	s^{-1}
$c_{cap,c}$	volumetric capacity of greenhouse air for carbon dioxide	4.1	M
$c_{cap,h}$	volumetric capacity of greenhouse air for humidity	4.1	M
$c_{cap,q}$	heat capacity of greenhouse air	30000	J m^{-2} °C^{-1}
U_c	supply rate of carbon dioxide		kg m^{-2} s^{-1}
U_q	energy supply by the heating system		W m^{-2}
U_v	ventilation rate		m s^{-1}
$\varphi_{vent,c}$	mass exchange of carbon dioxide through the vents		kg m^{-2} s^{-1}
$Q_{vent,q}$	energy exchange by ventilation and transmission through the cover		W m^{-2}
$Q_{rad,q}$	heat load by solar radiation		W m^{-2}
$\varphi_{transp,h}$	canopy transpiration		kg m^{-2} s^{-1}
$\varphi_{vent,h}$	mass exchange of humidity through the vents		kg m^{-2} s^{-1}
c_{leak}	leakage air exchange through greenhouse cover	0.75 10^{-4}	m s^{-1}
V_c	carbon dioxide concentration outside the greenhouse		kg m^{-3}
V_T	outdoor temperature		°C
V_h	outdoor humidity concentration		kg m^{-3}
$c_{cap,q,v}$	heat capacity per volume unit of greenhouse air	1290	J m^{-3} °C^{-1}
$c_{rad,q}$	heat load coefficient due to solar radiation	0.2	
$c_{v,pl,ai}$	canopy transpiration mass transfer coefficient	3.6 10^{-3}	m s^{-1}
$c_{v,1}$	parameter defining saturation water vapour pressure	9348	J m^{-3}
$c_{v,2}$	parameter defining saturation water vapour pressure	17.4	
$c_{v,3}$	parameter defining saturation water vapour pressure	239	°C
c_R	gas constant	8314	J^{-1} K^{-1} $kmol^{-1}$
$c_{T,abs}$	temperature in K at 0 °C	273.15	K
P	profit		$ m^{-2}
t_0	start time of optimization interval		s
t_f	end time of optimization interval		s
$c_{pri,1}$	parameter defining price of lettuce	0.954	$ m^{-2}
$c_{pri,2}$	parameter defining price of lettuce	8.48	$ kg^{-1}
c_q	price of heating energy	3.366 10^{-9}	$ J^{-1}
c_{co2}	costs of carbon dioxide	22.26 10^{-2}	$ kg^{-1}
c_v	price of ventilation	2.226 10^{-6}	$ m^{-3}
c_{el}	price of supplemental light	1.325 10^{-8}	$ J^{-1}
λ_s	co-state of crop dry weight		$ kg^{-1}
R_{Xh}	relative humidity		100%

Appendix B. Model synthesis

Applying the model of LED lighting to the greenhouse-crop model of van Henten (2003), the greenhouse model still has 3 states being greenhouse temperature X_T, humidity X_h, and CO_2 concentration X_c, while the crop still has only one state being crop dry weight X_d. The first-order differential equations representing the model are,

$$\frac{dX_d}{dt} = c_{\alpha\beta}\varphi_{phot,c} - c_{resp,d}X_d 2^{(0.1X_T-2.5)} \tag{6}$$

$$\frac{dX_c}{dt} = \frac{1}{c_{cap,c}}\left[-\varphi_{phot,c} + c_{resp,d}X_d 2^{(0.1X_T-2.5)} + U_c - \varphi_{vent,c}\right] \tag{7}$$

$$\frac{dX_T}{dt} = \frac{1}{c_{cap,q}}\left[U_q - Q_{vent,q} + Q_{rad,q}\right] \tag{8}$$

$$\frac{dX_h}{dt} = \frac{1}{c_{cap,h}}\left[\varphi_{transp,h} + \varphi_{vent,h}\right] \tag{9}$$

with,

$$\varphi_{phot,c} = \left(1 - e^{-c_{pl,d}X_d}\right) \times \frac{\left(c_{rad,phot}V_{rad} + c_{led,phot}U_l\right)\left(-c_{co_{2,1}}X_T^2 + c_{co_{2,2}}X_T - c_{co_{2,3}}\right)\left(X_c - c_\Gamma\right)}{\left(c_{rad,phot}V_{rad} + c_{led,phot}U_l\right) + \left(-c_{co_{2,1}}X_T^2 + c_{co_{2,2}}X_T - c_{co_{2,3}}\right)\left(X_c - c_\Gamma\right)} \tag{10}$$

$$\varphi_{vent,c} = \left(U_v + c_{leak}\right)\left(X_c - V_c\right) \tag{11}$$

$$Q_{vent,q} = \left(c_{cap,q,v}U_v + c_{ai,ou}\right)\left(X_T - V_T\right) \tag{12}$$

$$Q_{rad,q} = c_{rad,q}V_{rad} \tag{13}$$

$$\varphi_{transp,h} = \left(1 - e^{c_{pl,d}X_d}\right)c_{v,pl,ai}\left(\frac{c_{v,1}}{c_R\left(X_T + c_{T,abs}\right)}e^{c_{v,2}X_T/(X_T+c_{v,3})} - X_h\right) \tag{14}$$

$$\varphi_{vent,h} = \left(U_c + c_{leak}\right)\left(X_h - V_h\right). \tag{15}$$

To apply the two time-scale decomposition, a state-space representation of the model in which fast and slow parts of the dynamics are distinguished, is convenient. To that end define the system's full state vector, "slow state", and "fast state" in Eq. (16). Then full dynamics, slow dynamics, and fast dynamics are corresponding partial derivatives versus time.

$$x = \begin{bmatrix} x_s \\ x_f \end{bmatrix} = \begin{bmatrix} X_d \\ X_c \\ X_T \\ X_h \end{bmatrix}, x_s = X_d, x_f = \begin{bmatrix} X_c \\ X_T \\ X_h \end{bmatrix}. \tag{16}$$

The control input vector and external input vector are defined in Eq. (17).

$$u = \begin{bmatrix} U_c \\ U_q \\ U_v \\ U_l \end{bmatrix}, d = \begin{bmatrix} V_{rad} \\ V_T \\ V_c \\ V_h \end{bmatrix}. \tag{17}$$

Appendix C. Quasi steady state computation

Assuming X_T, X_h, and X_c to be in quasi steady state, explicit algebraic expressions representing these quasi steady states are derived below in terms of X_d as well as controls U_c, U_q, U_v, U_l and weather inputs V_{rad}, V_T, V_c, V_h.

Using the quasi steady state assumption $\dot{X}_T = 0$ we obtain from Eq. (8),

$$U_q - \underbrace{\left(c_{cap,q,v}U_v + c_{ai,ou}\right)}_{f_1}\left(X_T - V_T\right) + \underbrace{c_{rad,q}V_{rad}}_{f_2} = 0 \tag{18}$$

$$U_q - f_1\left(X_T - V_T\right) + f_2 = 0 \tag{19}$$

$$f_1 X_T = U_q + f_1 V_T + f_2 \tag{20}$$

$$X_T = \frac{U_q + f_1 V_T + f_2}{f_1}. \tag{21}$$

Quasi steady state X_T is then represented by Eq. (21).

To find steady state X_h first rewrite Eq. (15),

$$\varphi_{vent,h} = \underbrace{\left(U_v + c_{leak}\right)}_{U_{vcl}}\left(X_h - V_h\right) = U_{vcl}\left(X_h - V_h\right) \tag{22}$$

and next Eq. (14),

$$\varphi_{transp,h} = \underbrace{\left(1 - e^{c_{pl,d}X_d}\right)c_{v,pl,ai}}_{f_3}\left(\underbrace{\frac{c_{v,1}}{c_R\left(X_T + c_{T,abs}\right)}e^{c_{v,2}X_T/(X_T+c_{v,3})}}_{f_4} - X_h\right) = f_3\left(f_4 - X_h\right). \tag{23}$$

Using the quasi steady state assumption $\dot{X}_h = 0$ we obtain from Eq. (9),

$$\varphi_{transp,h} - \varphi_{vent,h} = 0 \tag{24}$$

$$f_3\left(f_4 - X_h\right) - U_{vcl}\left(X_h - V_h\right) = 0 \tag{25}$$

$$\left(f_3 + U_{vcl}\right)X_h = f_3 f_4 + U_{vcl}V_h \tag{26}$$

$$X_h = \frac{f_3 f_4 + U_{vcl}V_h}{f_3 + U_{vcl}}. \tag{27}$$

Quasi steady state X_h is then represented by Eq. (27) with X_T given by Eq. (21).

To find the quasi steady state X_c first rewrite Eq. (10),

$$\varphi_{phot,c} = \underbrace{\left(1 - e^{c_{pl,d}X_d}\right)}_{c_{Xd}} \times \frac{\underbrace{\left(c_{rad,phot}V_{rad} + c_{light,phot}U_l\right)}_{c_{Vr}}\left(-c_{CO2,1}X_T^2 + c_{CO2,2}X_T - c_{CO2,3}\right)\left(X_C - c_\Gamma\right)}{\underbrace{\left(c_{rad,phot}V_{rad} + c_{light,phot}U_l\right)}_{c_{Vr}} + \underbrace{\left(-c_{CO2,1}X_T^2 + c_{CO2,2}X_T - c_{CO2,3}\right)}_{c_T}\left(X_C - c_\Gamma\right)} \tag{28}$$

$$\varphi_{phot,c} = \frac{c_{Xd}c_{Vr}c_T\left(X_C - c_\Gamma\right)}{c_{Vr} + c_T\left(X_C - c_\Gamma\right)} \tag{29}$$

and Eq. (11),

$$\varphi_{vent,c} = \underbrace{\left(U_v + c_{leak}\right)}_{U_{vcl}}\left(X_c - V_c\right) = U_{vcl}\left(X_c - V_c\right) \tag{30}$$

$$c_{DU} = c_{resp,c}X_d 2^{(0.1X_T-2.5)} + U_c. \tag{31}$$

Using the quasi steady state assumption $\dot{X}_c = 0$ we obtain from Eq. (7),

$$\varphi_{phot,c} + \varphi_{vent,c} \underbrace{-c_{resp,c}X_d 2^{(0.1X_T-2.5)} - U_c}_{-c_{DU}} = 0 \tag{32}$$

$$\frac{c_{Xd}c_{Vr}c_T\left(X_c - c_\Gamma\right)}{c_{Vr} + c_T\left(X_c - c_\Gamma\right)} + U_{vcl}\left(X_c - V_c\right) - c_{DU} = 0 \tag{33}$$

$$c_{Xd}c_{Vr}c_T\left(X_c - c_\Gamma\right) + \left(U_{vcl}\left(X_c - V_c\right) - c_{DU}\right)\left(c_{Vr} + c_T\left(X_c - c_\Gamma\right)\right) = 0. \tag{34}$$

Quasi steady state X_c is then represented by Eq. (34) which is a quadratic equation,

$$aX_c^2 + bX_c + c = 0 \tag{35}$$

with,

$$a = U_{vcl}c_T \tag{36}$$

$$b = c_{Xd}c_{Vr}c_T + U_{vcl}c_{Vr} - U_{vcl}c_T c_\Gamma - U_{vcl}V_c c_T - c_{DU}c_T \tag{37}$$

$$c = -c_{X_d} c_{V_r} c_T c_\Gamma - U_{vcl} V_c c_{V_r} - U_{vcl} c_{DU} c_{V_r} + U_{vcl} V_c c_T c_\Gamma - c_{DU} c_{V_r} + c_{DU} c_T c_\Gamma. \quad (38)$$

References

Breuer, J. J. G., & van de Braak, N. J. (1989). Reference year for Dutch greenhouses. *Acta Horticulturae*, *248*, 101–108.

Dorais, M., & Gosselin, A. (2000). Physiological response of greenhouse vegetable crops to supplemental lighting. In *IV international ISHS symposium on artificial lighting, vol. 580* (pp. 59–67).

Engindeniz, S., & Tuzel, Y. (2006). Economic analysis of organic greenhouse lettuce production in Turkey. *Scientia Agricola*, *63*(3), 285–290.

Gonzalez, R., Rodriguez, F., Guzman, J. L., & Berenguel, M. (2014). Robust constrained economic receding horizon control applied to the two time-scale dynamics problem of a greenhouse. *Optimal Control Applications and Methods*, *35*(4), 435–453.

Heuvelink, E., & Challa, H. (1989). Dynamic optimization of artificial lighting in greenhouses. *Acta Horticulturae*, *260*, 401–412.

Ioslovich, I. (2009). Optimal control strategy for greenhouse lettuce: Incorporating supplemental lighting. *Biosystems Engineering*, *103*(1), 57–67.

Ioslovich, I., Gutman, P. O., & Linker, R. (2009). Hamilton–Jacobi–Bellman formalism for optimal climate control of greenhouse crop. *Automatica*, *45*(5), 1227–1231.

Lin, K. H., Huang, M. Y., Huang, W. D., Hsu, M. H., Yang, Z. W., & Yang, C. M. (2013). The effects of red, blue, and white light-emitting diodes on the growth, development, and edible quality of hydroponically grown lettuce (*Lactuca sativa L. var. capitata*). *Scientia Horticulturae*, *150*, 86–91.

Martineau, V., Lefsrud, M., Naznin, M. T., & Kopsell, D. A. (2012). Comparison of light-emitting diode and high-pressure sodium light treatments for hydroponics growth of Boston lettuce. *HortScience*, *47*(4), 477–482.

Pucheta, J. A., Schugurensky, C., Fullana, R., Patiño, H., & Kuchen, B. (2006). Optimal greenhouse control of tomato-seedling crops. *Computers and Electronics in Agriculture*, *50*(1), 70–82.

Ross, I. M., & Fahroo, F. (2004). Pseudospectral knotting methods for solving nonsmooth optimal control problems. *Journal of Guidance Control and Dynamics*, *27*(3), 397–405.

Rutquist, P. E., & Edvall, M. M. (2010). *Propt-matlab optimal control software*. Tomlab Optimization Inc.

Schmidt, M., Reinisch, K., Puta, H., Markert, A., Augustin, P., & Heissner, A. (1987). Determining climate strategies for greenhouse cucumber production by means of optimization. *IFAC Proceedings*, *20*(5), 345–350.

Seginer, I., van Straten, G., & van Beveren, P. J. (2017). Day-to-night heat storage in greenhouses: 2 sub-optimal solution for realistic weather. *Biosystems Engineering*, *161*, 188–199.

Singh, D., Basu, C., Meinhardt-Wollweber, M., & Roth, B. (2015). LEDs for energy efficient greenhouse lighting. *Renewable & Sustainable Energy Reviews*, *49*, 139–147.

Tap, R. F. (2000). *Economics-based optimal control of greenhouse tomato crop production* (Ph.D. thesis), Wageningen, The Netherlands: Wageningen University.

Tap, R. F., Van Willigenburg, L. G., & Van Straten, G. (1996). Receding horizon optimal control of greenhouse climate based on the lazy man weather prediction. *IFAC Proceedings Volumes*, *29*(1), 889–894.

van Beveren, P. J. M., Bontsema, J., van Straten, G., & van Henten, E. J. (2015). Optimal control of greenhouse climate using minimal energy and grower defined bounds. *Applied Energy*, *159*, 509–519.

van Henten, E. J. (1994). *Greenhouse climate management: an optimal control approach* (Ph.D. thesis), Wageningen, The Netherlands: Wageningen University.

van Henten, E. J. (2003). Sensitivity analysis of an optimal control problem in greenhouse climate management. *Biosystems Engineering*, *85*(3), 355–364.

van Henten, E. J., & Bontsema, J. (2009). Time-scale decomposition of an optimal control problem in greenhouse climate management. *Control Engineering Practice*, *17*(1), 88–96.

van Straten, G., van Willigenburg, L. G., & Tap, R. F. (2002). The significance of crop co-states for receding horizon optimal control of greenhouse climate. *Control Engineering Practice*, *10*(6), 625–632.

van Straten, G., van Willigenburg, G., van Henten, E., & van Ooteghem, R (2011). *Optimal control of greenhouse cultivation*. USA: CRC Press.

van Willigenburg, L. G., van Henten, E. J., & van Meurs, W. T. H. M. (2000). Three time-scale digital optimal receding horizon control of the climate in a greenhouse with a heat storage tank. *IFAC Proceedings*, *149–154*.

Velez-Ramirez, A. I., van Ieperen, W., Vreugdenhil, D., & Millenaar, F. F. (2011). Plants under continuous light. *Trends in Plant Science*, *16*(6), 310–318.

Wang, T., Wu, G., Chen, J., Cui, P., Chen, Z., Yan, Y., . . ., & Chen, H. (2017). Integration of solar technology to modern greenhouse in China: Current status, challenges and prospect. *Renewable & Sustainable Energy Reviews*, *70*, 1178–1188.

Xu, D., Du, S., & van Willigenburg, G. (2018a). Adaptive two time-scale receding horizon optimal control for greenhouse lettuce cultivation. *Computers and Electronics in Agriculture*, *146*, 93–103.

Xu, D., Du, S., & van Willigenburg, L. G. (2018b). Optimal control of Chinese solar greenhouse cultivation. *Biosystems Engineering*, *171*, 205–219.